Manufacturing Letters 22 (2019) 11–15

Contents lists available at ScienceDirect

Manufacturing Letters

journal homepage: www.elsevier.com/locate/mfglet

Autonomous in-situ correction of fused deposition modeling printers using computer vision and deep learning

Zeqing Jin, Zhizhou Zhang, Grace X. Gu *

Department of Mechanical Engineering, University of California, Berkeley, CA 94720, USA

ARTICLE INFO

Article history:
Received 29 June 2019
Received in revised form 25 August 2019
Accepted 18 September 2019
Available online 21 September 2019

Keywords:
Additive manufacturing
Fused modeling deposition
Computer vision
Deep learning
Convolutional neural networks

ABSTRACT

Fused deposition modeling, a widely used additive manufacturing process, currently faces challenges in printed part quality such as under-extrusion and over-extrusion. In this paper, a real-time monitoring and autonomous correction system is developed, where a deep learning model and a feedback loop is used to modify 3D-printing parameters iteratively and adaptively. Results show that our system is capable of detecting in-plane printing conditions and in-situ correct defects faster than the speed of a human's response. The fundamental elements in the framework proposed can be extended to various 3D-printing technologies to reliably fabricate high-performance materials in challenging environments without human interaction.

1. Introduction

Additive manufacturing has made huge strides in the past decades – it is now possible to fabricate multiscale, multimaterial and multifunctional designs previously deemed as impossible [1–6]. Fused deposition modeling (FDM) technology, which slices a model into thin layers where polymer filament is deposited to sketch the contour and fill the internal area layer-by-layer, is the most widely used additive manufacturing method for its low cost and ease of operation [7,8]. One limitation of FDM printers, however, involves in-plane printing issues such as under-extrusion and over-extrusion. These common issues are hard to eliminate and can accumulate to cause various print defects including undesired low modulus, low toughness, rough print surface, among others [9–11]. As a result, researchers have developed various approaches to improve print quality including tool path optimization [12,13] and mathematical modeling of printing parameters [14,15]. The settings deduced from these methods, however, are specific to a particular geometry or printer. Moreover, the approaches are not able to monitor or correct printing parameters in real-time. Currently, manually tuning printing parameters is still the most effective method to correct problems and obtain optimal print quality which requires extensive human experience and thus is not scalable to the industrial level.

Machine learning aided methods have been applied in recent years to a wide range of fields such as autonomous driving, face recognition, big data prediction, and materials design [16–20]. It has also been utilized in the field of additive manufacturing to inspect printing conditions [21]. Advanced methods such as combining three-dimensional digital image correlation (3D-DIC) with real-time monitoring for fused filament fabrication (FFF) printing has also been explored in literature [22]. However, the previous defect detection techniques either largely depend on the mathematical calculation based on the image or require expensive experimental equipment such as a DIC camera. Moreover, the previous systems require pauses or stops during the printing process to conduct any print judgments and are not capable of real-time correcting printing conditions. In this paper, we develop an autonomous system incorporating advanced machine learning algorithms to classify and detect printing issues and self-correct with optimal processing parameters to reliably 3D-print high-performance materials at fast rates and resolutions with enhanced dimensional accuracy. Specifically, our real-time monitoring and refining platform uses convolutional neural networks (CNN), which is a commonly used deep learning algorithm with images as input [23]. CNN transforms an image to an array of numbers that represent its category and the model that describes the mapping is trained and used to predict results for new unseen images. CNN algorithms are known for their capability to process and learn the spatial hierarchies of features in an image, while other classification methods oftentimes lose this information. Moreover, numerous models are attached to this algorithm such as AlexNet, Visual Geometry Group

* Corresponding author.
E-mail address: ggu@berkeley.edu (G.X. Gu).

https://doi.org/10.1016/j.mfglet.2019.09.005
2213-8463/

(VGG), Residual Network (ResNet); as our study focuses on input images with difficult to distinguish features, ResNet is used due to its superior performance on complex MNIST image data sets [24]. The paper is organized as follows. Section 2 discusses the experimental setup and methods used for the study. Section 3 shows the results and discussion of our training procedure and refinement performance. Section 4 summarizes the work and proposes future directions.

2. Experimental set-up and methods

Our machine learning based 3D-printing system consists of two parts: a post-training procedure and an in-situ real-time monitoring and refining section (Fig. 1a). In the first step, a CNN classification model is trained using a ResNet 50 architecture [24]. After the completion of the training period, during the 3D-printing process, real-time images are continuously fed into the model and classified to obtain the current printing condition. If an issue such as over-extrusion is detected, adjusting commands will be automatically executed to change printing parameters via an open-source 3D-printer controlling GUI. Embedded in our system is a continuous feedback detection and monitoring loop where images with new settings will iterate until a good quality condition is achieved.

2.1. Training data collection

In this work, all prints are produced by a PRUSA i3 MK3 FDM printer with polylactic acid (PLA) filament. An in-house designed 3D-printed camera mount is fixed on top of the extruder cap to suspend the camera and provides a fixed monitoring view during the printing process as seen in Fig. 2a. A 45° fan support is designed and printed with one of its corners removed to provide a clear view for monitoring. The camera model used in the system is a Logitech C270. Its front panel is removed so that the focal length can be adjusted for the best image quality at the print region beneath the nozzle. Videos are recorded and labeled with the corresponding categories: ‘Good-quality’, ‘Under-extrusion’ and ‘Over-extrusion’.

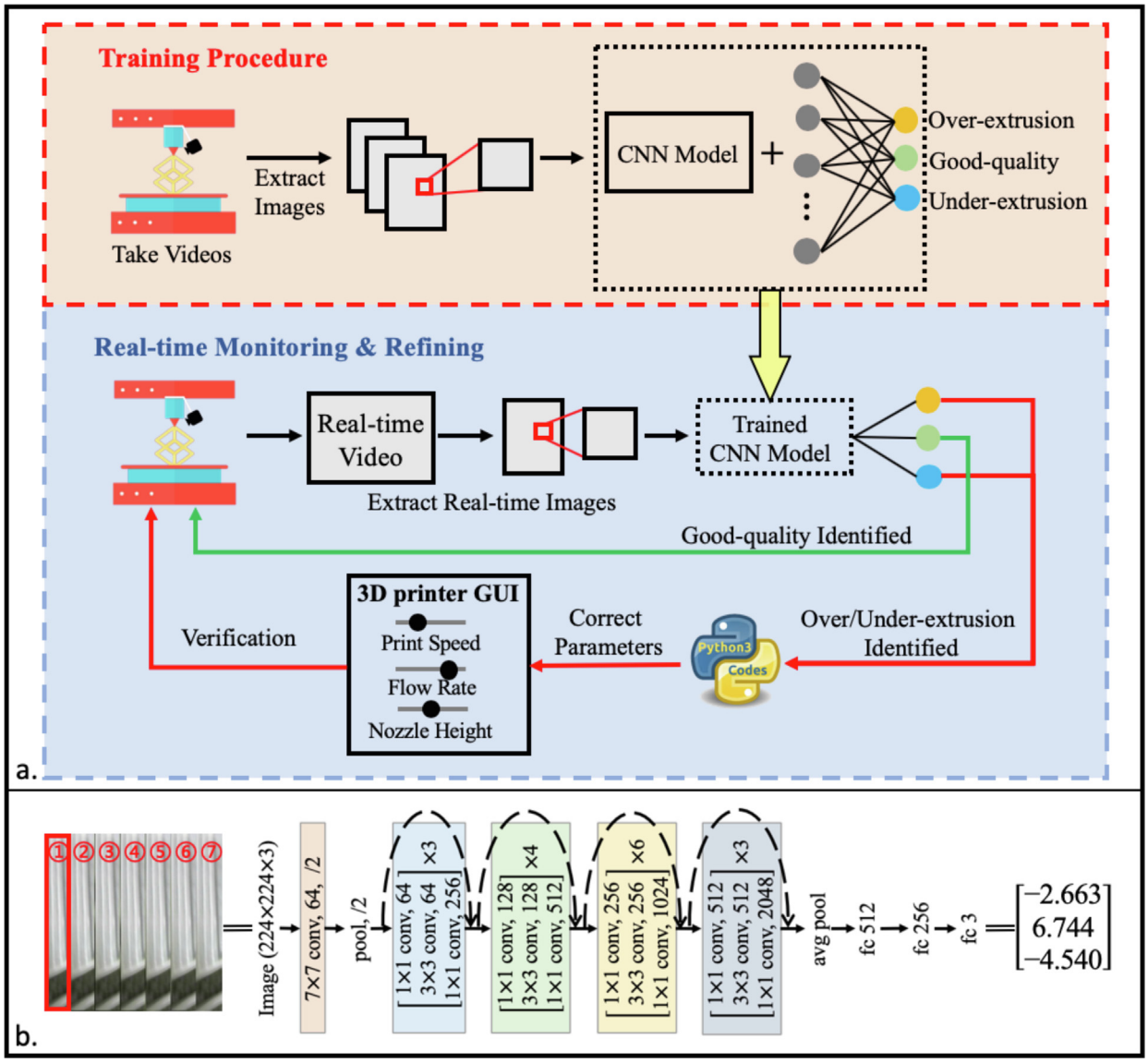

Fig. 1. (a) The system work flow is comprised of a training procedure, real-time monitoring, and refining component. A CNN model is trained in the first part and recorded. While monitoring, extracted real-time images will be fed into the saved model and then classified into three categories. Printing parameters will then be changed automatically when over or under-extrusion images are detected. (b) Modified CNN model is used in the system based on ResNet 50 architecture. Image is augmented six more times to match the model input size, and output of the model will be a vector with three elements.

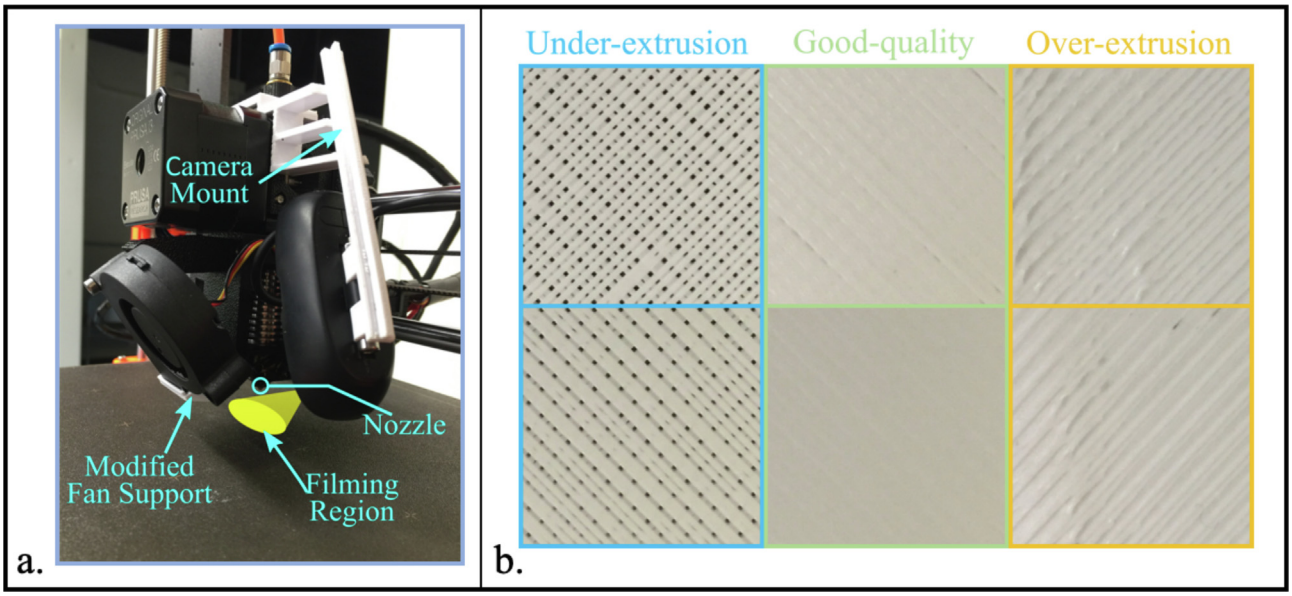

Fig. 2. (a) Experimental setup where a mount is designed and 3D-printed to attach the camera near the nozzle area. (b) Representative zoomed-in images for six 3D-printed blocks under different printing qualities categories of Under-extrusion, Good-quality, and Over-extrusion.

For each category, two levels of condition are generated by printing a five-layer block with size 50 mm × 50 mm × 1 mm. Representative topography 3D-printed samples for all three categories are shown in Fig. 2b.

2.2. Machine learning algorithm and training procedure

The CNN model that is used in the training process is a pre-trained ResNet 50 [25], which contains 16 residual blocks. In each block, there are three convolutional layers. With one more convolutional layer after input and another fully connected layer before output, there are a total of 50 layers in the pre-trained model. To better adapt our desired output with the model, the final layer is deleted and connected with another two layers to decrease the output size from 2048 to 3. Therefore, the output will be a vector of three by one (Fig. 1b). For each category, around 120,000 images are prepared, where 70% of them are randomly picked as training data and the rest of them are treated as validation or testing data.

2.3. Monitoring and self-correction

After the machine learning model is trained, it will be transferred into the monitoring and refining system. During the 3D-printing process, 20 real-time images are captured every 6 s and fed into the model. It is of note that this image acquisition rate is chosen to balance the accuracy of the testing result and the operational efficiency of the system. If fewer images are taken, the input data volume would be too small for the algorithm to compensate for the difficulties of accurately classifying the printing quality at boundary areas. On the other hand, if more images are considered, more computational operation and data accumulation time (delay time) will be needed. Additionally, this rate can also be modified to match the printing efficiency, which is controlled by the printing parameter of printing speed. In our experiments, the image acquisition rate is kept constant since the printing speed is unchanged. After obtaining these 20 classification results, the mode of them will be treated as one judgment of the current printing condition. This method is adopted to eliminate any noise image inputs and inaccurate classification that may occur when based solely on a single image. If five successive over or under-extrusion judgments appear, adjusting commands will be sent automatically via Pronterface [26], an open-source program, which can connect, control and communicate with the 3D-printer. Among different printing parameters such as print speed, flow rate, and nozzle height, in this work, the focus will be on the adjustment of flow rate. Flow rate is considered to be the major factor causing under and over-extrusion in 3D-printed materials since the imperfections are attributed to the lack of or too much flow of filaments. Other parameters such as print speed and nozzle height are not considered here due to their minor effects on in-plane issues; rather, these parameters play a larger role in inter-layer issues such as warping and delamination. After one correction command is sent, five following updated judgments will be recorded to decide whether the printing condition has improved. If the printing condition has not improved, further adjustments will be forwarded to the printer and the procedure will be repeated until five continuous Good-quality results are finally received by the system. Five consecutive judgments are employed here since the improvement process does not happen instantaneously. Less number of judgments do not provide enough time to reflect the transition period, while more judgments would be unnecessary if the condition has already reached a good quality condition.

3. Results and discussion

3.1. Validation of the model accuracy

The core component of the auto-correction system is a classification model which detects whether undesirable extrusion exists. Before training the model, further image processing is required for the collected video data. Full-sized images are transformed from the video at 20 frames per second. Since there are two perpendicular printing directions, in each direction, a fixed 32 × 224 rectangle window is extracted along the newly printed lines near the nozzle. In order to match the input image size of our machine learning model, each image is augmented six more times and concatenated together to form a 224 × 224 image (Fig. 3a). The input image has a physical width of 14 mm, which results in a resolution of 407 pixels per inch (ppi). In order to obtain an accurate model, the whole image data is trained for a sufficient number of epochs. The loss rate and accuracy against the epoch number are shown in Fig. 3b. The orange accuracy

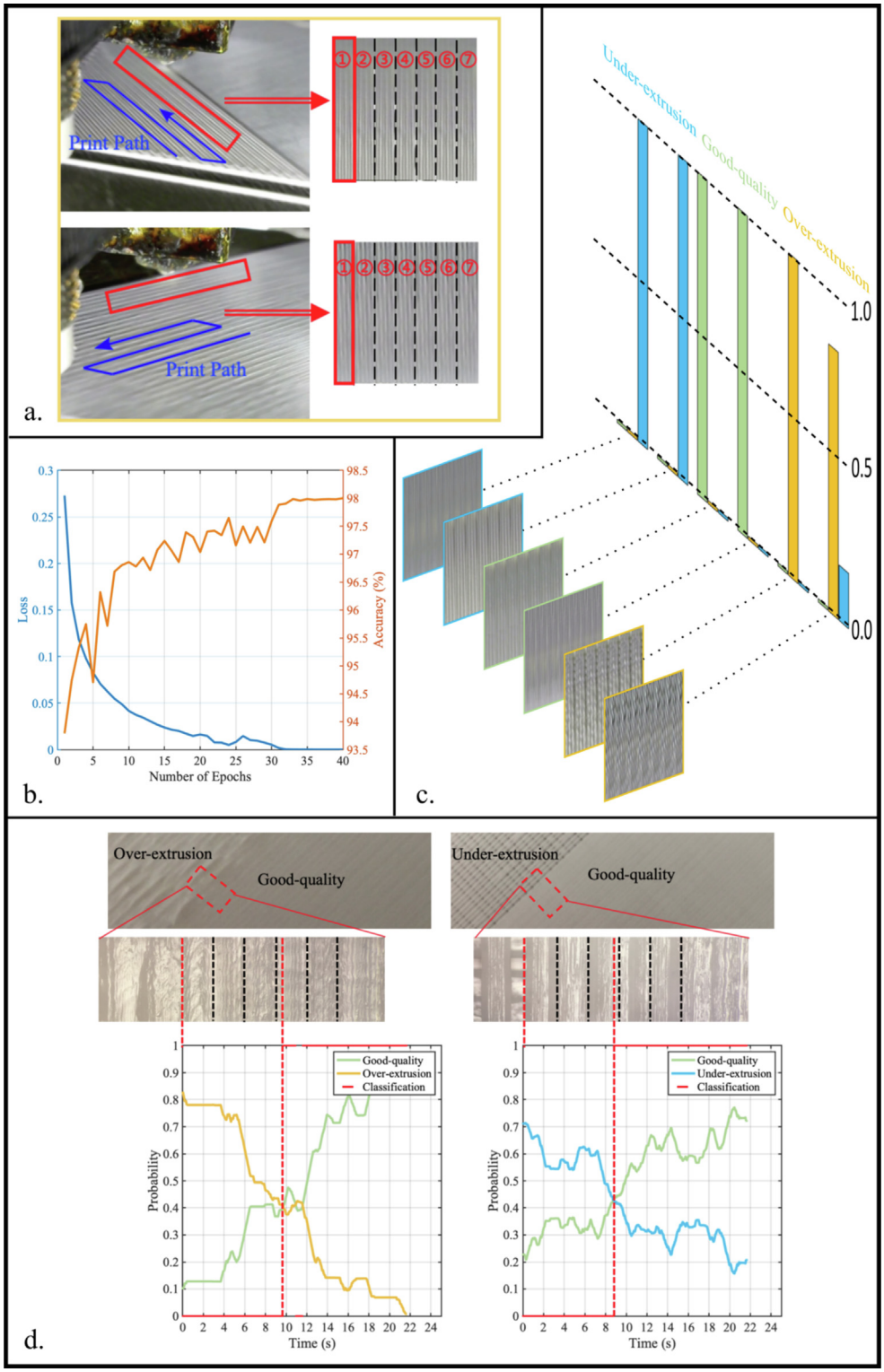

Fig. 3. (a) Two extraction windows are used correspondingly to two printing paths. Images are then augmented six more times for model input. (b) Training result of the CNN model shows the accuracy of the model on validation data set converges to 98% after 40 epochs of training. (c) Classification model validation and illustration of the probability of an image in three output categories. (d) Response results when detecting Over-extrusion and Under-extrusion conditions. Zoomed-in images are taken by microscope under 5× objective lens. Probability vs. time curves represent the probability of being certain category and are further binarized to red dots, which constitute horizontal lines. (For interpretation of the references to colour in this figure legend, the reader is referred to the web version of this article.)

curve converges to 98% after training for 40 epochs. Fig. 3c shows an example of the prediction of six images from the validation data set. The trained model takes an image as input and returns a 3×1 vector. The sum of each vector's three entries is normalized to 1 by a Softmax function such that they indicate the probability of an image to fall into the corresponding category. The final classification result of an image is determined by the highest column where blue, green, orange column represents the probability of Under-extrusion, Good-quality, and Over-extrusion respectively.

3.2. Efficiency of the correction system

In addition to accuracy, a quick response is equally essential for our platform to identify print quality variation and adjust its performance before continuing the print. Therefore, response time is measured when the printer corrects Under-extrusion or Over-extrusion conditions. During the printing process, when an Over- or Under-extrusion condition is detected, two transition states from bad to good are presented in Fig. 3d. At $t = 0$ s, marked by short vertical red dashed lines, the first Good-quality raster is printed. The curves show the probability of Good-quality and Over- or Under-extrusion images against time. As discussed previously, this probability is calculated by averaging the results of the images in the nearest 6 s to reduce the uncertainties from the photos captured at the margin of the print. When the value of good-quality probability surpasses another one, the collection of images will be further classified as 1, otherwise, 0, represented by horizontal red lines at the top or bottom edges of the two plots. The transitions from Over-extrusion and Under-extrusion to Good-quality are first detected by the monitoring system at $t = 9.8$ s and 8.6 s, which are marked by long red dash lines in the figure. The interval between every two neighboring black dash lines is 3 s which is the time needed to print one raster. Normally, it takes three rasters for human individuals to recognize improving print quality. Therefore, the model is capable of distinguishing the shift equally or even faster than a human can under both cases. Besides the detection delay of the monitoring system, the firmware delay (the time it takes for the extrusion motor to execute the Ponterface command and start to print modified rasters) is also a non-negligible component of the total response time. This firmware response time highly depends on the FDM printer and can vary from 12 to 18 s. The overall response time of the in-situ correction system is thus determined by the sum of the two delays.

4. Conclusions

In conclusion, we demonstrate an autonomous FDM 3D-printing platform which can in-situ monitor and adjust printing conditions based on a trained machine learning algorithm. Our algorithms are able to achieve above 98% accuracy in predicting the printed part status quality. Additionally, the response rate of the system reaches or even surpasses the human reaction and the model can recognize inferior images that humans will have a difficult time to distinguish with high accuracy. Future work for improving the system involves augmenting the training data set to make the model more robust, increasing the degrees of printing quality levels to make the refinement stage more effective, and separate models focusing on images at the boundary such as corners which often have limited training information during the assessment period. The framework thus developed in this paper to detect and self-correct systems in FDM technologies has the potential to be applied to other materials and manufacturing systems to reliably 3D-print high-performance materials especially in challenging environments without human interaction.

Declaration of Competing Interest

The authors declare that they have no known competing financial interests or personal relationships that could have appeared to influence the work reported in this paper.

Acknowledgements

The authors acknowledge support from the Extreme Science and Engineering Discovery Environment (XSEDE) by National Science Foundation grant number ACI-1548562. Additionally, the authors acknowledge support from an NVIDIA GPU Seed Grant, Johnson & Johnson WiSTEM2D Scholars Award, and an Amazon Research Award.

References

[1] Momeni FM, Mehdi Hassani NS, Liu X, Ni J. A review of 4D printing. Mater Des 2017;122:42–79. https://doi.org/10.1016/J.MATDES.2017.02.068.
[2] Zhang Z, Demir KG, Gu GX. Developments in 4D-printing: a review on current smart materials, technologies, and applications. Int J Smart Nano Mater 2019:1–20. https://doi.org/10.1080/19475411.2019.1591541.
[3] Jared BH, Aguilo MA, Beghini LL, Boyce BL, Clark BW, Cook A, et al. Additive manufacturing: toward holistic design. Scr Mater 2017;135:141–7. https://doi.org/10.1016/J.SCRIPTAMAT.2017.02.029.
[4] Melchels FPW, Domingos MAN, Klein TJ, Malda J, Bartolo PJ, Hutmacher DW. Additive manufacturing of tissues and organs. Prog Polym Sci 2012;37:1079–104. https://doi.org/10.1016/j.progpolymsci.2011.11.007.
[5] Gu GX, Takaffoli M, Buehler MJ. Hierarchically enhanced impact resistance of bioinspired composites. Adv Mater 2017;29:1–7. https://doi.org/10.1002/adma.201700060.
[6] Gu GX, Wettermark S, Buehler MJ. Algorithm-driven design of fracture resistant composite materials realized through additive manufacturing. Addit Manuf 2017;17:47–54. https://doi.org/10.1016/J.ADDMA.2017.07.002.
[7] Gibson I, Rosen D, Stucker B. Additive manufacturing technologies: 3D printing, rapid prototyping, and direct digital manufacturing, second edition. 2015. doi:10.1007/978-1-4939-2113-3.
[8] Gao W, Zhang Y, Ramanujan D, Ramani K, Chen Y, Williams CB, et al. The status, challenges, and future of additive manufacturing in engineering. CAD Comput Aided Des 2015;69:65–89. https://doi.org/10.1016/j.cad.2015.04.001.
[9] Bellehumeur C, Li L, Sun Q, Gu P. Modeling of bond formation between polymer filaments in the fused deposition modeling process. J Manuf Process 2004;6:170–8. https://doi.org/10.1016/S1526-6125(04)70071-7.
[10] Hart KR, Wetzel ED. Fracture behavior of additively manufactured acrylonitrile butadiene styrene (ABS) materials. Eng Fract Mech 2017;177:1–13. https://doi.org/10.1016/J.ENGFRACMECH.2017.03.028.
[11] Ahn D, Kweon J-H, Kwon S, Song J, Lee S. Representation of surface roughness in fused deposition modeling. J Mater Process Technol 2009;209:5593–600. https://doi.org/10.1016/J.JMATPROTEC.2009.05.016.
[12] Dreifus G, Rapone B, Bowers J, Chen X, Hart AJ, Krishnamoorthy B. A framework for tool path optimization in fused filament fabrication. In: Proc. 1st Annu. ACM Symp. Comput. Fabr. - SCF '17, New York. New York, USA: ACM Press; 2017. p. 1–2. https://doi.org/10.1145/3083157.3092883.
[13] Chakraborty D, Aneesh Reddy B, Roy Choudhury A. Extruder path generation for curved layer fused deposition modeling. CAD Comput Aided Des 2008;40:235–43. https://doi.org/10.1016/j.cad.2007.10.014.
[14] Mohamed OA, Masood SH, Bhowmik JL. Optimization of fused deposition modeling process parameters for dimensional accuracy using I-optimality criterion. Measurement 2016;81:174–96. https://doi.org/10.1016/J.MEASUREMENT.2015.12.011.
[15] Peng A, Xiao X, Yue R. Process parameter optimization for fused deposition modeling using response surface methodology combined with fuzzy inference system. Int J Adv Manuf Technol 2014;73:87–100. https://doi.org/10.1007/s00170-014-5796-5.
[16] Chen CT, Gu GX. Effect of constituent materials on composite performance: exploring design strategies via machine learning. Adv Theory Simulations 2019;2:1900056. https://doi.org/10.1002/adts.201900056.
[17] Yang C, Kim Y, Ryu S, Gu GX. Using convolutional neural networks to predict composite properties beyond the elastic limit. MRS Commun 2019:1–9. https://doi.org/10.1557/mrc.2019.49.
[18] Pilania G, Wang C, Jiang X, Rajasekaran S, Ramprasad R. Accelerating materials property predictions using machine learning. Sci Rep 2013;3:2810. https://doi.org/10.1038/srep02810.
[19] LeCun Y, Bengio Y, Hinton G. Deep learning. Nature 2015;521:436–44. https://doi.org/10.1038/nature14539.
[20] Gu GX, Chen CT, Richmond DJ, Buehler MJ. Bioinspired hierarchical composite design using machine learning: simulation, additive manufacturing, and experiment. Mater Horizons 2018;5:939–45. https://doi.org/10.1039/C8MH00653A.
[21] Delli U, Chang S. Automated process monitoring in 3D printing using supervised machine learning. Procedia Manuf 2018;26:865–70. https://doi.org/10.1016/J.PROMFG.2018.07.111.
[22] Holzmond O, Li X. In situ real time defect detection of 3D printed parts. Addit Manuf 2017;17:135–42. https://doi.org/10.1016/J.ADDMA.2017.08.003.
[23] LeCun Y, Haffner P, Bottou L, Bengio Y. Object recognition with gradient-based learning. Berlin, Heidelberg: Springer; 1999. p. 319–45. https://doi.org/10.1007/3-540-46805-6_19.
[24] He K, Zhang X, Ren S, Sun J. Deep residual learning for image recognition 2015.
[25] torchvision.models.resnet — PyTorch master documentation n.d. https://pytorch.org/docs/stable/_modules/torchvision/models/resnet.html#resnet50 (accessed June 23, 2019).
[26] GitHub - kliment/Printrun: Pronterface, Pronsole, and Printcore - Pure Python 3d printing host software n.d. https://github.com/kliment/Printrun (accessed June 23, 2019).